

Neutron-diffraction structure in potassium near the [011] and [022] Bragg points

S. A. Werner

Department of Physics and Astronomy, University of Missouri–Columbia, Columbia, Missouri 65211

A. W. Overhauser

Department of Physics, Purdue University, West Lafayette, Indiana 47907

T. M. Giebultowicz

*Department of Physics, University of Notre Dame, Notre Dame, Indiana 46556
and The National Institute of Standards and Technology, Gaithersburg, Maryland 20899*

(Received 20 April 1989)

Neutron diffraction from a stress-free crystal of potassium shows no increase in its ($\sim 0.03^\circ$) mosaic width after repeated cycling between 4 and 300 K. Furthermore, no temperature-dependent, Huang-type diffuse scattering near [011] and [022] was found. Properties such as these, indicative of thermally-induced plastic deformation, were reported for the potassium crystals studied by Pintschovius *et al.* and by Blaschko *et al.* Their data also exhibited a sample-caused background as much as 100 times larger than our stress-free crystal. Using 2.35-Å-wavelength neutrons and tight collimation, we find that the satellite structure near [011] retains the same spacing near [022]. The structure cannot be attributed to a double-scattering artifact, which requires a spacing proportional to $\tan\theta_B$. The data are consistent with a charge-density-wave interpretation.

We present new neutron-diffraction data on the structure near the [011] and [022] Bragg points in potassium that are consistent with our previous data and conclusions.¹ A critical review is given of other neutron-scattering data on K, recently reported by Pintschovius *et al.*² (hereafter called PB1) and by Blaschko *et al.*³ (hereafter called PB2). We believe that the quality of the K crystals used in PB1 and PB2 was so poor that charge-density-wave (CDW) satellites could probably not have been observed. The structure reported in PB1 was indeed caused by a double-scattering artifact,⁴ a possibility which we had entertained,⁵ but were able to exclude for our experiments on the basis of not observing this structure in a Si test crystal.⁶ The cause of the artifacts in PB1 was an extraordinarily large diffuse scattering generated by sample imperfections. This spurious scattering caused a background that was 100 times larger in the PB2 experiment than that found in the high-quality, stress-free crystal studied in this work and in Ref. 1.

We interpreted our original data¹ as being due to CDW satellites in a $(0\bar{1}1)$ diffraction plane near [011], as shown by the black dots in Fig. 1. There are other satellite locations which, however, are not expected to be observable because either their intensities are too weak or they lie too close to the mosaic sphere passing through each Bragg point. A CDW satellite is surrounded by an ellipsoidal cloud of phason diffuse scattering⁷ indicated by the shaded regions of Fig. 1. The centroids of these inelastic scattering phason clouds is shifted towards the [011] Bragg point and away from the location of the elastic CDW satellite points. The reason for this is shown schematically in Fig. 2. The interaction between the

phason modes originating from the CDW satellite point Q and the acoustic phasons originating from the Bragg point G gives rise to a branch splitting. The vertical width of these curves is proportional to the square of the amplitudes of these modes. Even at 4 K, about 90% of the integrated intensity resides in the phason cloud.¹ Since phason scattering is inelastic, the apparent location of the satellite will depend on both the energy and momentum resolution of the triple-axis neutron spectrometer. This effect is illustrated schematically by curves A and B in Fig. 1. This explains why the satellite locations appear to shift with incident-neutron wavelength.¹

Our new data involve scanning the structures surrounding both the [022] and [011] Bragg points as shown in Fig. 3. A neutron wavelength, $\lambda = 2.35 \text{ \AA}$, was chosen so that both regions could be studied with comparable resolution. (The [022] point cannot be reached with $\lambda = 4.08 \text{ \AA}$ neutrons.) If the observed structure were caused by a double-scattering artifact, then the transverse spacing between the observed peaks (satellites) would be 2.5 times larger near [022] than near [011]. The reason is that the angle between the double-scattering streaks is equal to $2\theta_B$.⁴ However, we find the spacing between the peaks in scans transverse to the $\langle 011 \rangle$ axis near [022] and [011] to be equal, which is the expected result for CDW satellites. Representative scans at $k = 0.980$ and 1.980 are shown in Fig. 4. Unfortunately, the resolution is not quite good enough to separate the structures into three separated peaks. We fitted the data for the two scans to three Lorentzian peaks, each having a width identical to the measured transverse widths of the [011] and [022] Bragg peaks, respectively. The relative in-

egrated intensity of the fitted peaks near [022] to those near [011] is 7.6. For a CDW modulation this ratio should be 4.6, which is obtained from assuming that the CDW satellite cross section, along with its phason cloud, is proportional to the convolution of the scattering cross section with the four-dimensional resolution function. The resolution ellipsoid near [022] overlaps a larger fraction of the intense region of the phason cloud than near [011]. This effect is difficult to model accurately, but likely accounts for the larger intensity observed near [022].

We have investigated the temperature dependence of the diffraction structure. For T sufficiently high so that the phason temperature factor^{8,9} of the elastic component is small, the integrated intensity of the phason cloud should be independent of T . As T increases, the shape of the phason cloud will change gradually, since the convo-

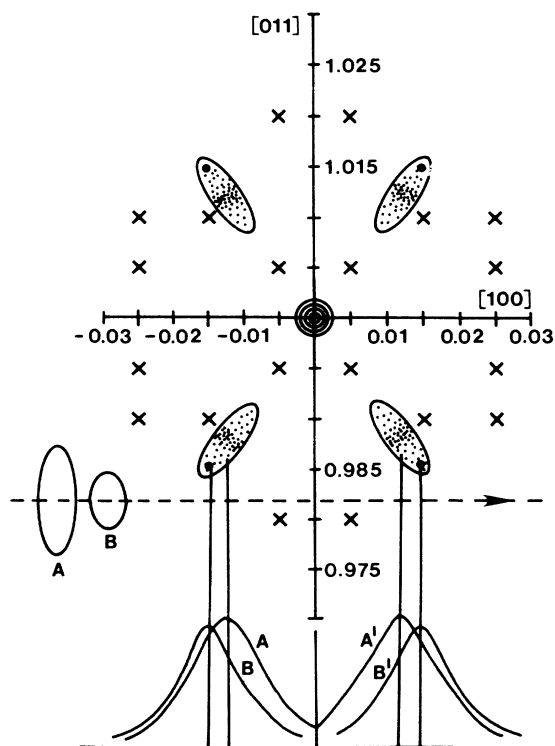


FIG. 1. Upper half: map of the $(0\bar{1}1)$ diffraction plane surrounding the [011] Bragg point. The large dots at ± 0.015 , 0.985, and ± 1.015 are the principal CDW satellite locations. The diffuse phason clouds surrounding these satellites are asymmetric (as expected from Fig. 2). The \times 's are the locations of other satellites which are either too weak to be observed or are too near the [100] axis to be isolated from the [011] mosaic tail. Lower half: schematic diffraction profiles for a transverse scan (dashed line) along the trajectory $[h, 0.982, 0.982]$. The apparent shift of the profiles (A, A' to B, B') when the neutron wavelength is changed from 2.35 Å (resolution ellipsoid A) to 4.08 Å (resolution ellipsoid B) arises from the altered convolution with the phason diffuse scattering.

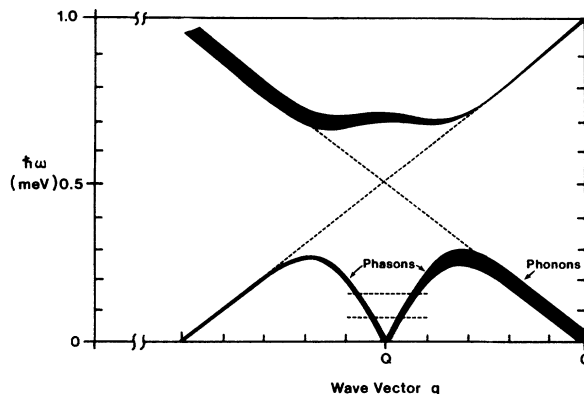


FIG. 2. Phason and amplitude-mode spectra near a CDW satellite at $q=Q$. The diagonal dashed lines are the phonon dispersion curves (appropriately translated) that would be present if there were no CDW. The vertical widths of the solid curves are proportional to the neutron-scattering cross section for each mode (but do not include the Bose-Einstein thermal factors). The maximum frequency of the phason spectrum is ~ 0.3 meV for K. The horizontal dashed lines depict energy resolutions for two neutron wavelengths and indicate why phason clouds appear to shift with neutron wavelength.

lution of multiple-phason events leads to a diffusivelike growth. Accordingly, the apparent amplitude of the CDW-related scattering can either increase, decrease, or remain constant with increasing T , depending on the location of the scan line in reciprocal space relative to the satellite center. We have found for a transverse scan $(h, 1.975, 1.975)$ that the structure has about the same

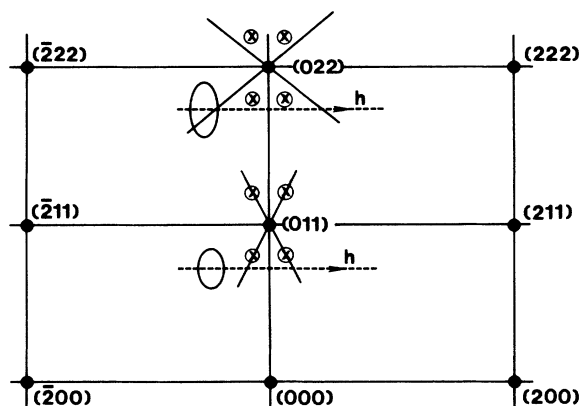


FIG. 3. Schematic map of the $(0\bar{1}1)$ diffraction plane near the [011] and [022] Bragg points. The diagonal lines through [011] and [022] depict the orientation of streaks due to possible double-scattering artifacts. The angle of these lines, relative to $\langle 011 \rangle$, is the Bragg angle θ_B . When the resolution ellipsoids are convolved with the CDW satellites—the four \times 's surrounding [011] and [022]—the satellite spacings along the indicated transverse scans will be the same near [011] and [022]. The spacings between double-scattering artifacts will be proportional to $\tan \theta_B$.

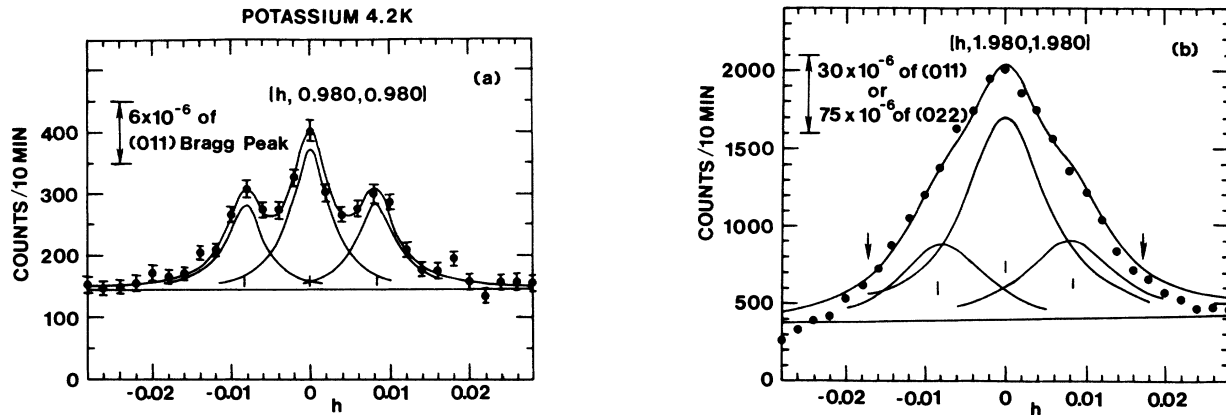


FIG. 4. (a) Transverse scan of the satellites in K near [011] for $\lambda = 2.35$ and $T = 4.2^\circ$ K. The width of the Lorentzian components ($2\Gamma = 0.0056$) was determined by a fit to the [011] rocking-curve profile; (b) transverse scan near [022]. The width of the Lorentzian components ($2\Gamma = 0.0124$) was fixed by the [022] rocking-curve profile. The arrows mark the locations of potential double-scattering artifacts. The central components in (a) and (b) arise from the overlap of the resolution ellipsoid with the nearby Bragg peaks. The monochromator and analyzer are PG (002). The incident beam contains a pyrolytic graphite (PG) filter between the monochromator and the reactor end of the Soller collimator. The collimations are $10'-12'-12'-21'$. The energy resolution is 0.28 meV.

amplitude at 4 and 78 K. Further experiments are necessary to explore the scan dependence of this (possibly surprising) result.

Since K undergoes a 5% volume contraction on cooling to 4 K, it is essential to mount the crystal in a manner that prevents plastic deformation. We achieved this requirement by supporting our crystal between compressed-quartz wool at each end, within a He-gas-

filled aluminum capsule. Our data have never shown any signs of crystal deformation and the crystal has retained its sharp mosaic width after more than 50 cool-downs to 4 K. A recent study¹⁰ of this crystal with 50 kV x rays showed that the mosaic width is 0.03° . By contrast, the crystals of PB1 and PB2 suffered incremental increases in mosaic width on each cool-down, a behavior which can only be attributed to plastic deformation. The PB1 and

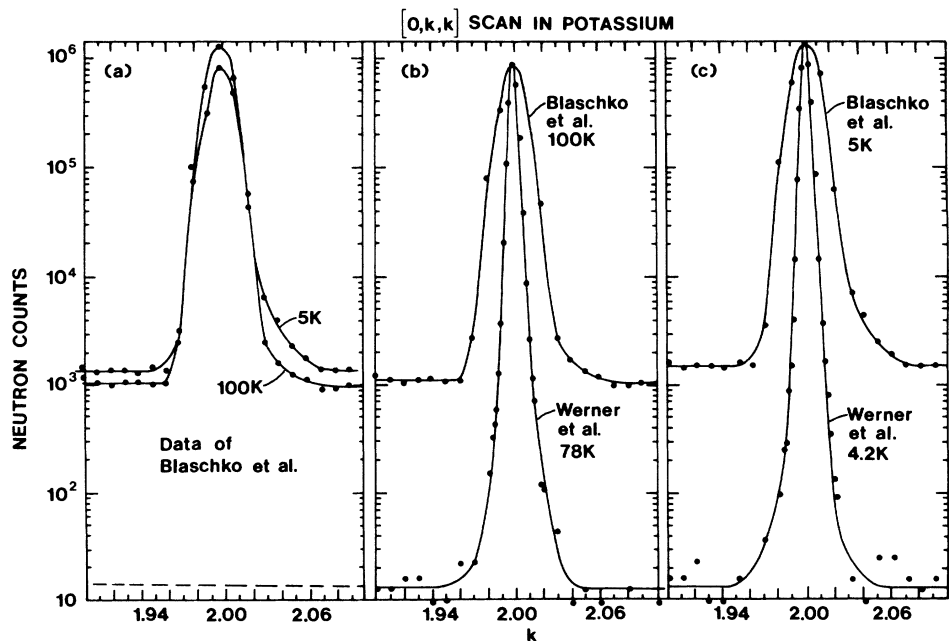


FIG. 5. Longitudinal scans through the [022] Bragg point of K using $\lambda = 2.35 \text{ \AA}$ neutrons. Note the logarithmic vertical scale. (a) Data of Blaschko *et al.* (Ref. 3) which show a large increase in diffuse scattering near the base of the [022] on cooling from 100 to 5 K; (b) comparison of the ~ 100 K data of Blaschko *et al.* with that of Werner *et al.* (this paper) normalized to a common peak height. Note the 100-fold disparity in diffuse background scattering; (c) comparison of the ~ 5 K data of Blaschko *et al.* with that of Werner *et al.*, normalized to a common peak height. The disparity in diffuse scattering is larger than that in (b), since there is no change in background for our K crystal.

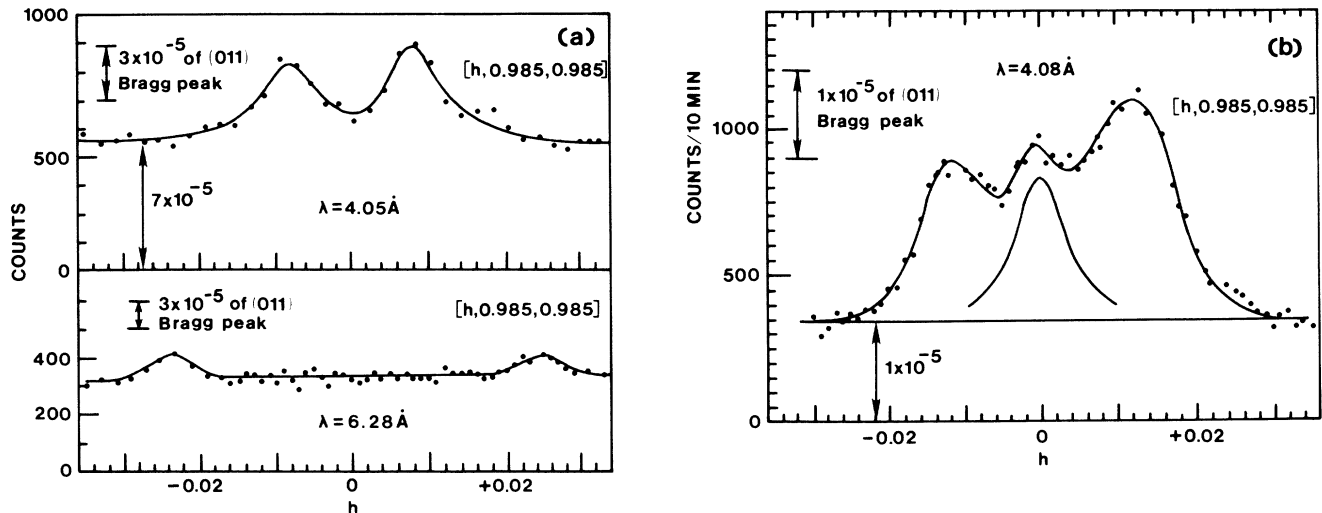


FIG. 6. Transverse scans near the [011] Bragg peak of K; (a) data of Pintschovius *et al.* (Ref. 2) for $\lambda = 4.05$ and 6.28 \AA , which show structure caused by a double-scattering artifact; (b) data of Giebultowicz *et al.* (Ref. 1). Note the factor-of-7 difference in background levels.

PB2 experiments at 5 K were done on a crystal with a mosaic spread of $0.3^\circ - 0.5^\circ$, more than 10 times the mosaic width of our crystal. The large increases in diffuse scattering near the base of the [011] and [022] Bragg reflections reported by PB2 [and shown in Fig. 5(a)] during cool-down from 100 to 5 K shows the consequence of additional plastic deformation. This increase, which alone exceeds our total background by a factor of ~ 50 , can be ascribed to newly generated dislocations. The cause(s) of the plastic deformation in the crystals of PB1 and PB2 is either the specimen clamp, KOH degradation, or hydrocarbon contamination left from crystal growth. A comparison of longitudinal scans through [022] at 78 and 4 K in our crystal with the data of PB2 is shown in Figs. 5(b) and 5(c). Note the factor-of-100 difference in the background levels between our data and that of PB2.

The extinction factor ϵ of the [011] Bragg peak is an important quantity, and is needed to calibrate satellite intensities and to compare data from different samples. For $\lambda = 4.08 \text{ \AA}$, we found $\epsilon = 1/7$. This was done by normalizing the scattered intensity to the incident beam intensity using a National Bureau of Standards (NBS) calibrated fission chamber,¹¹ neutron photographic images of the diffracted beam to determine the effective sample scattering volume, and a wide-open detector to accept the full Bragg-diffracted beam. Since the samples used by PB1 and PB2 had mosaic widths 10 times larger than ours, and since their samples were subjected to severe plastic deformation with each cool-down, the only reasonable hypothesis is that $\epsilon \sim 1$ for those specimens.¹² We show in Fig. 6 a comparison of the data of PB1 and of Giebultowicz *et al.*¹ At comparable wavelengths (4.05 and 4.08 \AA) the ratio of the background to the [011] Bragg peak

intensity is seven times higher in PB1 than for our data (Ref. 1). Furthermore, if ϵ is in fact 1 for PB1 as we surmise, their sample-caused background would be 50 times higher than ours, thus obviating the possibility of PB1 observing the same structure reported in our original paper.

It seems appropriate to emphasize again⁶ that the symmetry of this structure about the [011] Bragg point is incompatible with scattering caused by martensitic embryos. (Such embryos could lead to two diffuse peaks on the [000] side of [011] but not (also) to two peaks on the [022] side of [011].)

CDW satellites can also be studied with x-ray diffraction. However, an attempt to find satellites in potassium by You *et al.* failed.¹³ They employed 1.05 \AA synchrotron radiation, which has an absorption length of $200 \mu\text{m}$. Since the Bragg angle for K [011] is 8.16° , their diffracting volume was within $10 \mu\text{m}$ of the sample surface. It has been established that surface elastic strain can dramatically alter the electrical resistivity of potassium. Such effects have been studied in wires¹⁴ and in spheres¹⁵ (the so-called oil-drop effect¹⁶). The presumption is that strain can alter the CDW Q direction and, as a consequence, CDW satellites could be smeared out. Potassium samples inevitably have a thick KOH surface layer which will create thermal stress near the surface. 50 keV x rays should be used in a search for CDW satellites since a bulk sample 2 cm thick can then be penetrated.

We are grateful to the National Science Foundation for financial support.

- ¹T. M. Giebultowicz, A. W. Overhauser, and S. A. Werner, *Phys. Rev. Lett.* **56**, 1485 (1986).
- ²L. Pintschovius, O. Blaschko, G. Krexner, M. de Podesta, and R. Currat, *Phys. Rev. B* **35**, 9330 (1987).
- ³O. Blaschko, M. de Podesta, and L. Pintschovius, *Phys. Rev. B* **37**, 4258 (1988).
- ⁴S. A. Werner and M. Arif, *Acta Crystallogr. Sect. A* **44**, 383 (1988).
- ⁵T. M. Giebultowicz, A. W. Overhauser, and S. A. Werner, *Phys. Rev. Lett.* **56**, 2228 (1986).
- ⁶S. A. Werner, T. M. Giebultowicz, and A. W. Overhauser, *Phys. Scr.* **T19**, 266 (1988). The last paragraph of this paper was intended to begin "One may *not* come to the conclusion . . ." instead of "one may *now* come to the conclusion. . ."
- ⁷A. W. Overhauser, *Phys. Rev. B* **34**, 7362 (1986).
- ⁸A. W. Overhauser, *Phys. Rev. B* **3**, 3172 (1971).
- ⁹G. F. Giuliani and A. W. Overhauser, *Phys. Rev. B* **23**, 3737 (1981).
- ¹⁰R. Colella and Quin Zhao (unpublished).
- ¹¹The help of Dr. D. Gilliam in the incident-beam-intensity calibration is appreciated.
- ¹²PB1 states that $\epsilon \approx 1/40$ for their sample as measured by normalizing to a powder diffraction line. We are not familiar with that normalization procedure, which obviously requires a detailed understanding of the spectrometer vertical resolution function.
- ¹³Hoydoo You, J. D. Axe, Dietmar Hohlwein, and J. B. Hastings, *Phys. Rev. B* **35**, 9333 (1987).
- ¹⁴H. Taub, R. L. Schmidt, B. W. Maxfield, and R. Bowers, *Phys. Rev. B* **4**, 1134 (1971).
- ¹⁵F. W. Holroyd and W. R. Datars, *Can. J. Phys.* **53**, 2517 (1975).
- ¹⁶A. W. Overhauser, *Adv. Phys.* **27**, 343 (1978).